Published in final edited form as:
Vasc Dis Prev. 2008 August 1; 5(3): 200–210. doi:10.2174/156727008785133809.

C_6-Ceramide-Coated Catheters Promote Re-Endothelialization of Stretch-Injured Arteries

Sean M. O'Neill[1], **Dina K. Olympia**[1], **Todd E. Fox**[1], **J. Tony Brown**[1], **Thomas C. Stover**[1], **Kristy L. Houck**[1], **Ronald Wilson**[2], **Peter Waybill**[3], **Mark Kozak**[4], **Steven W. Levison**[5], **Norbert Weber**[6], **Linda M. Karavodin**[7], and **Mark Kester**[1,*]

[1] Department of Pharmacology, Penn State College of Medicine, Hershey, PA

[2] Department of Comparative Medicine, Penn State College of Medicine, Hershey, PA

[3] Department of Radiology, Penn State College of Medicine, Hershey, PA

[4] Department of Medicine, Penn State College of Medicine, Hershey, PA

[5] Department of Neurosciences, New Jersey Medical School, Newark, NJ

[6] Department of Chemistry and Chemical Biology, Rutgers University, NJ

[7] REVA Medical, Inc., San Diego, CA, USA

Abstract

Objective—Drug eluting stents have recently been associated with the increased risk of adverse thrombogenic events and/or late luminal loss, which is highly associated with incomplete re-endothelialization. The increased risks behoove the design of alternative delivery modalities and/or drugs that do not compromise the re-endotheliaization process. The objective of the present study is to elucidate the biological mechanism(s) by which non-stent-based delivery modalities for the anti-proliferative lipid metabolite, C_6-ceramide, could lead to a reduction in arterial injury after angioplasty.

Results—Immunohistochemical studies in rabbit and porcine models suggest that C_6-ceramide-coated balloon catheters limit arterial stenosis without inhibiting endothelial wound healing responses. Specifically, C_6-ceramide-coated balloon catheters reduce internal elastica injury with a corresponding reduction in medial fracture length in a 28-day porcine coronary artery stretch model. In addition, C_6-ceramide decreases the formation of the fibrin matrix to possibly augment the subsequent wound healing response. We hypothesized that differential metabolism of exogenous ceramide by coronary endothelial and smooth muscle cells could explain the apparent discrepancy between the anti-proliferative actions of ceramide and the pro-wound healing responses of ceramide. Human coronary artery endothelial cells (HCAEC), in contrast to human coronary artery smooth muscle cells (HCASMC), preferentially express ceramide kinase and form ceramide-1-phosphate, which promotes endothelial cell survival.

Conclusion—Differential metabolism of ceramide between HCASMC and HCAEC offers a mechanism by which ceramide preferentially limits smooth muscle cell growth, in the presence of active wound healing. The combinatorial ability of ceramide to limit vascular smooth muscle proliferation and promote re-endothelialization, offers the potential for C_6-ceramide-coated catheters to serve as adjuncts to stent-based modalities or as a stand-alone treatment.

*Address correspondence to this author at the 500 University Dr. Hershey, PA 17033, USA; Tel: (717)531-8964; Fax: (717)531-5013; mxk38@psu.edu.

INTRODUCTION

Despite the overwhelming successes with drug-eluting stents, treatment of stenotic injury in patients with complex, tortuous, or diffuse lesions, especially in diabetic patients, is still limited [1,[2]]. Moreover, drug-eluting stents have recently fallen back into controversy due to the risk of increased thrombotic events and/or late luminal loss [3,[4]]. In addition, the potentially problematic use of long term clopidogrel treatment in certain populations as well as the cost of stent-based therapies have led to re-evaluation of drug eluting stents [5]. As the most useful predictor of thrombotic events with drug-eluting stents is incomplete re-endothelialization [6], therapies that maintain active wound healing while limiting neointimal hyperplasia may be a potentially useful therapeutic strategy. To this end, local delivery *via* a balloon catheter of a lipophilic drug that limits intimal hyperplasia while promoting endothelial coverage of the balloon-induced injury is an attractive option. Utilizing non-stent-based drug delivery modalities, such as a drug-coated percutaneous transluminal coronary angioplasty balloon catheter, may offer an alternative treatment option for patients with diffuse injury or in-stent restenosis. In fact, a paclitaxel-coated therapeutic balloon has been shown to be a novel method for prevention of restenosis in a porcine overstretch stent model [7], as well as for treatment of human coronary in-stent restenosis [8].

We previously demonstrated that cell-permeable ceramide, which inhibits growth factor-mediated signaling cascades, reduced neointimal hyperplasia without systemic complications in a rabbit carotid model of stretch injury [9]. Despite demonstration of the vascular anti-proliferative actions of ceramide-coated balloons, the effects on other components of restenosis, including re-endothelialization, remodeling, and inflammation, have not been demonstrated. The present study suggests that C_6-ceramide-coated balloons limit arterial stenosis without inhibiting endothelial wound healing responses, further implicating the use of ceramide-coated therapeutic balloons for the treatment of diffuse vascular stenosis as seen in diabetic patients. Moreover, the use of ceramide-coated therapeutic balloons has the potential to promote active endothelial wound healing not only in coronary arteries, but also, in larger diameter arteries.

Materials and Methods

All animal studies were approved by the Pennsylvania State University College of Medicine Institutional Animal Care and Use Committee and conform to the *Guide for the Care and Use of Laboratory Animals* published by the US National Institutes of Health (NIH Publication No. 85-23, revised 1996).

Porcine Angioplasty Surgery

Mixed breed domestic heparinized (100 mg/kg) male swine weighing between 45 – 56 kg were used in the studies. Access to the arterial system was made through a femoral cut-down and balloon catheters were guided and deployed under fluoroscopy. Appropriate sizing of selected arterials was calculated from x- ray film. 3.3, 5, and 8 Fr balloon dilation catheters were used and sized in the coronary (left anterior descending or circumflex), renal, and iliac arteries, respectively. Sham-operated arteries were used in all experiments. Balloon catheters were inflated three times to manufacturers specification (8–10 ATM) for 30 sec intervals. One month after angioplasty, swine were assessed radiologically and then euthanized. Arteries were removed, fixed, and processed for hematoxylin/eosin staining. Experiments were performed at LyChron, Inc. (Mountain View, CA), as well as Penn State College of Medicine. Similar results were obtained at both facilities. Histochemical analyses for the experiments run at LyChron were contracted to the Armed Forces Institute of Pathology (Washington, DC).

Cholesterol Fed Rabbit Angioplasty Surgery

We now extend our previous work in normal-fed rabbits [9], performing quantitative morphometric analyses of carotid artery intimal hyperplasia and medial hypertrophy in angioplastied arteries from 2% cholesterol fed New Zealand white (NZW) rabbit (RSI, Mocksville, NC). The left carotid artery was used as a sham-treated control in all studies. There were no significant differences between sham control, vehicle control, or ceramide-treated arteries in terms of either tissue wet weight or cellular protein content. Other controls included ligation of the external carotid artery without balloon angioplasty, which did not develop neointimal or thrombolytic events in the common carotid.

Catheter Coating Preparation

3.3, 5, and 8 Fr balloon dilation catheters were coated with lipid gels (C_6-ceramide (0.5% C_6-ceramide [Avanti Polar Lipids, Alabaster, Alabama] in 90:10 ethanol: DMSO) or dihydro-C_6-ceramide (0.5% dihydro-C_6-ceramide [BIOMOL International, Plymouth Meeting, PA] in 90:10 ethanol: DMSO) or vehicle (90:10 ethanol: DMSO)), in double blinded protocol.

Histochemistry and Immunohistochemistry

Hematoxylin and eosin staining was performed according to our previously published work. [9] For Sudan IV staining, fixed sections were immersed in a 1% Sudan IV in a 1:1 70% ethanol: acetone solution for 5 min. Immunohistochemical staining for PDGF-ββ staining utilized a goat polyclonal antibody for PDGF-ββ (R&D Systems, Minneapolis, MN) and streptavidin horseradish peroxidase (Amersham, Chicago, IL) for visualization.

Proliferation and Apoptosis Assays

^{3}H-thymidine incorporation [10] and caspase 3/7 activities [11] were used as surrogate markers to assess proliferation and apoptosis, respectively, in human coronary artery smooth muscle cells (HCASMC) (Cascade Biologics, Portland, Oregon) and human coronary artery endothelial cells (HCAEC) (Cell Applications, Inc, San Diego, California). Ceramide metabolites were delivered in 80–90 nm diameter liposomal vesicles as described [11]. Control liposomes were made up without ceramide metabolites, but contained the same amount of total lipids.

Fibrinogen Adsorption Assay

Poly(DTE carbonate), a well-characterized tyrosine-derived polymer [12], was mixed with paclitaxel or C_6-ceramide in a 90:10 ratio using tetrahydrofuran (THF) as a solvent. The spin-coating of the polymer mix on gold-coated quartz crystals and the detection of polymer-adsorbed fibrinogen were performed using a Quartz Crystal Microbalance with Dissipation monitoring (QCM-D) as previously described [13]. Human fibrinogen at a concentration of 3 mg/mL was used for all experiments.

Quantitative Real-Time RT-PCR

Total RNA was isolated using Qiagen RNeasy Mini Kit (Qiagen, Inc, Valencia, CA) according to manufacturer's protocol. RNA quantity and quality were assessed using the Agilent 2100 Bioanalyzer with the RNA 6000 Nano Assay (Agilent, Palo Alto, CA). cDNA synthesis was performed on total RNA using Superscript III Reverse Transcriptase (Invitrogen, Carlsbad, CA) and quantitative PCR on samples using previously described methods [14]. Detection used the 7900HT Sequence Detection System (Applied Biosystems), 384-well optical plates, and Assay-On-Demand (Applied Biosystems, Foster City, CA) gene specific primers and probes [15], maintained at Penn State College of Medicine Functional Genomics Core Facilities. The relative quantities of neutral and alkaline ceramidase, sphingosine kinase-1,

ceramide kinase, galactosylceramide synthase, and glucosylceramide synthase mRNA expression were calculated using ABI SDS 2.2.2 RQ software and the $2^{-\Delta\Delta Ct}$ analysis method [16] with β-actin as the endogenous control. Final results are given as relative expression normalized to vehicle treated HCAEC samples.

Lipid Quantification by Mass Spectroscopy

Sphingolipids from HCASMC and HCAEC cells were analyzed by electrospray ionization-tandem mass spectrometry (ESI-MS/MS) based on the method described by Merrill *et al.* [17] and modified by us [18]. The mass spectrometry data was collected using an ABI 4000 Q Trap (Applied Biosystems, Foster City, CA) mass spectrometer equipped with a turbo ion spray source. The peak areas for the different sphingolipid subspecies were compared with that of the internal standards.

Toxicology and Toxicokinetic Studies

Toxicology studies were performed *via* contract services at Redford Laboratories, AR using 6–10 week Sprague Dawley rats or 6-month Beagle dogs. The test article was a formulation of 1.5 mg/mL C_6-ceramide in 2% ethanol, 3% PVP, 8% Chromophor EL and 87% water. Dosing solutions were prepared as specified by Pharmatek Laboratories, San Diego or AAI International, Charleston SC; containing GMP grade C_6-ceramide obtained from Avanti Polar Lipids (Alabaster AL). In the multiple dose dog studies, the only adverse finding noted was a dose-dependent recovery period noted in both ceramide and vehicle control groups (prostration, increased saliva, reddened skin), which resolved rapidly, suggesting the transient adverse effects of the high dose ethanol vehicle, not related to the test article. Necropsy, standard histology, clinical chemistry, and coagulation findings were normal.

Statistical Analysis

The results are expressed as mean ± standard error of at least three independent experiments. Probability (p) values ≤ 0.05 (Student's t-test) were considered to indicate statistically significant differences. Results of the quantitative real-time RT-PCR were compared using one-way ANOVA.

RESULTS

C_6-Ceramide-Therapeutic Balloons Reduce Internal Elastica Injury with a Corresponding Reduction in Medial Fracture Length

C_6-ceramide's putative role in the prevention of injury-induced stenosis has been based on its well-documented ability to induce cell cycle arrest in VSM cells [10,[19]] and to limit neointimal hyperplasia in a balloon injury rabbit carotid artery model [9]. We have extended these previously reported data by investigating C_6-ceramide therapeutic balloons in a one-month porcine model of stretch injury. Initially, we evaluated coronary artery injury and resultant stenosis in a 1.3-1 overstretch porcine coronary artery mode. As shown in Fig. (**1A**), C_6-ceramide therapeutic balloons reduced internal elastica injury with a corresponding reduction in fracture sites and in medial fracture length. Moreover, stenotic injury at the fracture sites was significantly reduced. In these n = 6–9 separate, double-blinded, randomized porcine experiments, all of the C_6-ceramide-treated coronary vessels responded with less proliferation and less injury as compared to the corresponding vehicle balloon control arteries. Both medial fracture length and stenosis were reduced by over 50% with ceramide treatment (Fig. (**1B**)). As controls, pre- and post-artery diameter, injury ratio, and device diameter per compliance values did not change as a function of ceramide treatment (Fig. (**1C**)). These data support the contention that local acute delivery of C_6-ceramide to injured arteries limits smooth muscle proliferation as a possible consequence of diminishing proliferative signaling cascades [9],

diminishing arterial trauma/injury, or promoting wound healing (re-endothelialization) responses.

We next confirmed these porcine coronary experiments with additional studies investigating the effects of C_6-therapeutic balloons on other porcine arterial beds. In Fig. (**1D**), we show that C_6-ceramide therapeutic balloons limit stenosis by greater than 50% in renal and iliac vessels. Again, in these n = 5 porcine two-week experiments, coronary vessel stenosis was also reduced by acute, direct C_6-treatment. Histochemical (Fig. (**1E**)) and radiological (Fig. (**1F**)) assessments show significant stenosis and occlusion in the control iliac tree after angioplasty that was limited by C_6-ceramide treatment.

C_6-Ceramide-Coated Balloon Limits Arterial Stenosis without Inhibiting Endothelial Wound-Healing Responses

It appears that overstretch with the C_6-therapuetic balloon resulted in re-endothelialization of the traumatized artery (Fig. (**1E**)). To confirm augmented re-endothelialization of damaged, over-stretched arteries with C_6-ceramide *in vivo*, we utilized the rabbit carotid artery angioplasty model. Three days after angioplasty, we demonstrate that endothelial cells express elevated levels of PDGF-ββ, a hallmark of a healing endothelial lining, after treatment with ceramide-treated, but not control DMSO-treated, balloon catheters (Fig. (**1G**)). These data support a role for ceramide-enhanced wound healing to limit stenotic injury.

To begin to probe the mechanism(s) of diminished arterial stenosis after angioplasty with the C_6-therapeutic balloon despite active wound healing, we utilized an *in vit*ro approach. We directly compared the effects of C_6-ceramide upon HCASMC and HCAEC. As controls, other anti-proliferative therapeutic agents for the vasculature such as rapamycin and paclitaxel were investigated. The ED_{50} value for growth inhibition of HCASMC by a 24 hr treatment of C_6-ceramide was approximately 100 nmol/L (Fig. (**2A**)). Thus, this concentration of ceramide was utilized in further experimentation. 100 nmol/L C_6-ceramide significantly inhibited HCASMC growth (Fig. (**2B**)), but not HCAEC growth (Fig. (**2C**)), after a 24 hr treatment. As controls, paclitaxel, at an equivalent 100 nmol/L concentration, inhibited both HCASMC and HCAEC proliferation, while rapamycin inhibited HCAEC, but not HCASMC proliferation.

HCAEC and HCASMC Differentially Express mRNA for Ceramide Metabolizing Enzymes

The mechanistic explanation for the differential effect of exogenous C_6-ceramide upon vascular smooth muscle and endothelial cells may involve ceramide metabolism. Specifically, we hypothesize that HCAEC preferentially metabolizes exogenous ceramide into ceramide-1-phopshate (C-1-P), a pro-mitogenic, anti-apoptotic second messenger (Fig. (**3A**)). Unlike ceramide, C-1-P has been shown to be pro-mitogenic [20]. Using quantitative real-time polymerase chain reaction analysis (QRT-PCR) to measure gene expression of ceramide metabolic enzymes, we now provide evidence for ceramide metabolism in the diametric responses of vascular endothelial and smooth muscle cells to C_6-ceramide treatment. HCASMC cultures had significantly lower mRNA levels of ceramide kinase, the enzyme that forms ceramide-1-phosphate (C-1-P), relative to levels in HCAEC cell cultures (Fig. (**3B**)). The relative levels of ceramide kinase in HCAEC cultures were over twice that of HCASMC cultures. Therefore, HCAEC may have the enhanced capacity to metabolize ceramide into ceramide-1-phosphate (C-1-P). Interestingly, mRNA levels of ceramidases (neutral and alkaline) and sphingosine kinase, the enzymes responsible for the formation of pro-mitogenic sphingosine-1-phosphate (S-1-P), did not significantly differ between the HCAEC and HCASMC cultures (data not shown).

In addition, QRT-PCR analysis showed HCASMC cultures expressed significantly higher mRNA levels of galactosylceramide synthase and glucosylceramide synthase, relative to levels

expressed in HCAEC cultures (Fig. (**3C–3D**)). In HCASMC cultures, relative mRNA levels of these enzymes that are responsible for the generation of galactosyl- and glucosylceramide species were both over three times the respective mRNA levels in HCAEC cultures. Glycosylated ceramide metabolites are often less bioactive than native ceramide. Taken together, HCAEC and HCASMC differentially express mRNAs for ceramide metabolizing enzymes, which may offer an explanation for the dichotomous actions of exogenous C_6-ceramide upon vascular tissues.

Ceramide-1-Phosphate Accumulates in Human Coronary Artery Endothelial Cells

Using HPLC/MS/MS analysis, we next examined if the metabolism of exogenously delivered C_6-ceramide to HCASMC and HCAEC correlates with the differences between sphingolipid enzyme mRNA levels in the two cell lines. Consistent with the higher expression of ceramide kinase mRNA found in HCAEC compared to HCASMC, levels of C-1-P in HCAEC are approximately twice the levels found in HCASMC (Table 1) after treatment with C_6-ceramide. Furthermore, following treatment with C_6-ceramide, galactosyl- and glucosylceramide species, which were quantified together as cerebroside mass, were 6-fold higher in HCASMC (Table 1). This correlates well with levels of galactosyl- and glucosylceramide synthase mRNA in HCASMC, which are, as previously mentioned, over 3 times the levels found in HCAEC. Although expression of sphingosine kinase mRNA did not differ significantly between HCAEC and HCASMC, mass levels of mitogenic S-1-P in HCAEC were 50% greater than levels in HCASMC (data not shown), further supporting the ability of C6-ceramide to inhibit SMC growth while promoting re-endothelialization of the wounded artery. No significant mass differences between the cell types were observed for other sphingolipids, including total ceramides, sphingomyelin, and sphingosine (Table 1, data not shown).

C-1-P Enhances VEGF-Induced Endothelial Cell Survival

Our studies suggest that HCAEC have the capacity and ability to generate endogenous C-1-P and/or to metabolize exogenously applied ceramide into C-1-P. Although C-1-P has been shown to be proliferative and/or pro-inflammatory in certain cell types, its effects on HCAEC have not been validated. Exogenously delivered C_8–C-1-P in liposomal formulations, at a concentration of 1 μmol/L, neither directly induced proliferation in HCAEC nor significantly enhanced VEGF-induced HCAEC proliferation as determined *via* ^{3}H-thymidine incorporation (Fig. (**4A**)). In contrast, exogenously delivered C_8–C-1-P (1 μmol/L) promoted endothelial cell survival by attenuating serum deprivation-induced apoptosis in HCAEC, using caspase 3/7 activities as a marker of apoptosis (Fig. (**4B**)). Moreover, under serum-deprived conditions, C_8–C-1-P modestly enhanced VEGF induced endothelial cell survival (Fig. (**4B**)). Thus, the physiological correlate of elevated ceramide kinase mRNA expression and elevated C-1-P mass in HCAEC may be diminished apoptotic potential, consistent with enhanced wound healing responses to exogenous ceramide.

C_6-Ceramide Modifies the Formation of the Fibrin Matrix

Enhanced fibrinogen deposition and persistent fibrin formation often is associated with thrombus formation as well as a lack of efficient endothelial wound healing responses. Interestingly, surface-adsorbed fibrinogen reportedly initiates the acute inflammatory response to implanted polymers [21]. We, thus, evaluated the effects of C_6-ceramide to modify the formation of the fibrin matrix and, in part, to regulate the early wound healing response. We examined fibrinogen adsorption to C_6-ceramide coated films and demonstrated that fibrinogen binding was significantly reduced by approximately 35–40% *vs* the bare film, while a paclitaxel coating had little or no effect (Fig. (**5**)).

In the next series of experiments, we investigated *in vivo* this putative anti-thrombogenic, negative remodeling mechanism of action for ceramide. We utilized a cholesterol-fed rabbit

model of hyperlipidemia. In this model, carotid arteries responded to angioplasty with positive remodeling, thrombosis, and neointimal hyperplasia. We demonstrated that this model has increased levels of cholesterol and LDL, with diminished concentrations of HDL (Fig. (**6A–6C**)). Moreover, Sudan 4 staining revealed enhanced lipid accumulation within the neointimal and thrombogenic core of the angioplastied carotid arteries (Fig. (**6D**)). C_6-ceramide therapeutic balloon treatment reduced the degree of positive remodeling and thrombosis at the site of injury (Fig. (**6E–6G**)), which correlated with a significant reduction of stenosis (Fig. (**6I**)). Dihydro-C_6-ceramide, an inactive ceramide analogue, did not reduce thrombogenesis or stenosis within the damaged artery (Fig. (**6H**)). Taken together, the ability of ceramide to modify the formation of the fibrin matrix may regulate the subsequent early healing response and diminish thrombotic events, suggesting an ancillary mechanism by which ceramide contributes to normal healing.

C_6-Ceramide is Non-Toxic in Animal Models

Non-clinical toxicity and pharmacokinetic profiles have been analyzed for C6-ceramide in four single-dose studies (rat and dog), two multiple-dose sub-chronic studies (rat [28 days] and dog [14 days]), and two pharmacokinetic analyses (rat and dog).

At doses up to 15 mg/kg in rats and 7.5 mg/kg in dogs there were no drug-related adverse effects based on clinical observations, body weights, feed consumption, hematological parameters, clinical chemistry, electrocardiograms, gross pathology, organ weights, and histopathology (data not shown). There was also no evidence of mutagenicity, assayed by microbial cell mutagenesis, mammalian cell mutagenesis, and the mouse bone marrow micronucleus test with C_6-ceramide formulations up to 1000 mg/kg (BioReliance Rockville, MD).

In pharmacokinetic intravenous injection studies, the maximal plasma concentration of C_6-ceramide (T_{max}) was achieved within 2 min of injection. There was good dose proportionality of the maximum plasma concentration of C_6-ceramide (C_{max}) and area under the curve (AUC_{all}). Elimination from the plasma was biphasic with a short half-life in the distribution phase (around 3–5 min in rats and 4–7 min in dogs) and a longer half-life in the terminal phase (about 1.5 h in rats and between 1.5 – 1.83 h in dogs). Maximum tolerated and therapeutic doses of C_6-ceramide were determined for rat and dog; therapeutic ranges of doses were determined for pig and rabbit. We evaluated the non-clinical toxicity of C_6-ceramide as it relates to a potential human dose of approximately 150 μg given as a coating on an intracoronary device. Table 2 presents the maximum tolerated C_6-ceramide concentrations in two species, the conversion to the human equivalent dose, and the multiple of the expected clinical dose as a measure of the safety of this compound. In all cases, the expected clinical dose of ceramide used on the therapeutic balloon is three orders of magnitude below the maximum tolerated concentration of ceramide.

DISCUSSION

Even though ceramides are usually considered anti-proliferative or pro-apoptotic mediators, tissue specific metabolism can alter the pleiotropic responses to exogenous ceramide analogues. For example, fibroblasts often respond to exogenous ceramide with a proliferative response [22]. In the present study, human vascular endothelial cells, in contrast to human vascular smooth muscle cells, responded to ceramide with minimal growth arrest *in vitro* and pro-wound healing responses *in vivo*. The reason for this dichotomy between VSM and endothelial cell responses could be at the level of differential metabolism of exogenously applied C_6-ceramide.

We have now shown that ceramide kinase mRNA expression and C-1-P mass (in C6-ceramide treated cells) are elevated in HCAEC compared to HCASMC. As opposed to the general anti-proliferative effects of ceramide, C-1-P has been shown to be pro-mitogenic and promote cell survival in several cell types [20]. We have extended these studies to show that C-1-P augmented VEGF induced cell survival in HCAEC. In this way, exogenous ceramide analogues can be preferentially metabolized into ceramide-1-phosphate in endothelial cells, possibly promoting a pro-wound healing response consistent with the lack of prothrombotic events *in vitro* (Fig. (**5**)) and *in vivo* (Fig. (**6**)). It is of interest that the mRNA and protein levels of the S-1-P receptor (subtype 1) are also over-expressed in coronary artery endothelial cells *vs* coronary artery smooth muscle cells [23], and that ceramidases are actively released by murine endothelial cells [24], these findings are consistent with an increased endothelial wound healing response mediated by phosphorylated ceramide metabolites.

Another metabolic difference between HCASMC and HCAEC is at the level of cerebrosides. We have shown that HCASMC have increased expression of glucosyl- and galactosylceramide synthases, correlating with an increased mass of cerebroside species. The role of cerebrosides and/or cerebroside metabolites in VSM is somewhat controversial. Lactosylceramide has been shown to be proliferative in VSM [25] while glucosyl-and galactosylceramide species have been shown to be somewhat less bioactive than ceramide species [26]. Regardless, basal human coronary artery smooth muscle cells metabolized exogenous ceramide into these glycosphinogolipid metabolites and not into the highly pro-mitogenic phosphorylated C-1-P and S-1-P species.

The preferential metabolism of ceramide to C-1-P by HCAEC may explain how exogenous ceramide is a mediator of VSM cell cycle arrest or senescence [9,[10]] while simultaneously promoting endothelial cell wound healing responses. Another mechanism that may be responsible for pro-wound healing responses at the site of injury may involve a reduction of fibrinogen absorption/deposition on injured arteries. The ability of ceramide to modify the formation of the fibrin matrix may contribute to diminished thrombus formation as well as enhanced growth factor- or C-1-P-induced re-endothelialization. In fact, C-1-P has recently been shown to directly activate phospholipase A_2-induced arachidonate release, an important mediator in controlled inflammatory responses such as re-endothelialization or wound healing. Other reports have also commented upon the mechanisms by which ceramide can limit vascular injury. For instance, intravenous or intracisternal delivery of cell permeable ceramide analogues reduces infarct size in SHR rats *via* induction of tolerance to ischemia [27].

Even though our studies indicate that exogenous ceramide may reduce thrombogenic or fibrogenic events in hypercholesterolemic models, its role in developing atherosclerotic lesions is still somewhat controversial. Ceramide has been shown to be a component of LDL particles [28], yet it is now believed that ceramide metabolites, including S-1-P, lead to foam cell development, atherogenesis, and thrombogenesis [29,[30]]. In fact, ceramide, itself, may also be beneficial in limiting atherosclerosis through ceramide-dependent eNOS expression [31] and the inhibition of TNF-induced adhesion protein expression [32], subsequent to HDL binding to endothelial scavenger receptors. Ceramide also inhibits gene transcription of sterol regulatory element binding proteins to mediate a physiological feedback mechanism to lower cholesterol biosynthesis [33]. Taken together, the promotion of negative remodeling and/or wound healing are events consistent with the limitation of proliferation, thrombogenesis and fibrogenesis observed in our ceramide-treated hypercholesterolemic rabbit model of arterial injury.

Despite successes with drug eluting stents (DES), limiting restenosis from 20 to 9%, analyses of cost-effectiveness have raised some issues concerning populations and diseases suitable for these devices as well as their ultimate effects upon patient mortality [34]. In fact, the Basel

Stent Cost Effectiveness Trial (BASKET) study has recently concluded that cost-effectiveness issues should limit DES to elderly populations (>65 years) with lesions greater than 20 mm or arteries thinner than 2.5 mm [35]. Moreover, the use of DES for tortuous, disperse, bifurcated, and multiple vascular lesions, especially in diabetes or peripheral arterial disease, may be limited by definition. The fact that ceramide-coated balloon catheters greater than 8 mm limit stenosis in porcine iliac and renal arteries argue for the use of this modality for diffuse injury in large non-coronary beds. Our lipid-based coating process for balloon catheters requires no polymer matrix or X-ray/contrast medium substances, which could augment secondary thrombus formation or inflammatory processes. In addition, the coating process offers a homogeneous surface coating suitable for delivery of hydrophobic substances such as C_6-ceramide. This may offer an advantage over stent coatings where these types of drugs may accumulate within or near stent struts, leading to undesirable toxicological side effects due to the drug or the polymer. Advantages of coating conventional PCTA catheters go beyond economical considerations; PCTA catheters offer enhanced flexibility as well as the ability to treat lesions beyond the stent coverage area or to treat in-stent restenosis. These considerations have recently been exploited by the Paclitaxel balloon coating system [7,[8],[36]], where inhibition of restenosis can occur independent of chronic delivery *via* DES implantation [8].

In conclusion, the use of a therapeutic balloon as an adjunct to traditional and drug-eluting stent therapy or as a stand-alone modality has direct clinical applicability and may meet unmet medical conditions associated with pro-inflammatory, pro-mitogenic arterial or venous (SVG) lesions. Moreover, the delivery of an agent that limits neointimal hyperplasia while promoting endothelial wound healing responses directly addresses the major health concern with drug eluting stents.

Acknowledgments

NIH Grants HL66371 and HL076789 to MK, and EB003057-02 and SBIR Grant HLO75925-01 to NW supported this work. Mark Kester, Ph.D. participated in a related but separate project sponsored in part by REVA Medical, Inc. We would like to acknowledge the Functional Genomics Core Facilities at the Penn State College of Medicine for their assistance in quantitative PCR analyses. We thank Bruce Stanley and Pingqi Dai of the Proteomics/Mass Spectrometry Core Facility of the Section of Research Resources, Penn State College of Medicine for assistance with lipodomic experiments. We would also like to thank Joan Zeltinger, Ph.D. and Joachim Kohn, Ph.D. who provided insights into the fibrinogen studies and Ray Rothstein for immunohistochemical analysis. As well, we would like to thank Robert Schultz, Ph.D. and Jessica Earley, who helped guide the porcine studies. Finally, we thank Annie Kozak for her help with editing.

References

1. Elezi S, Dibra A, Schömig A, Kastrati A. Current drug-eluting stents in complex patients and lesions. Minerva Cardioangiol 2006;54:5–22. [PubMed: 16467738]
2. Nielsen TT, Botker HE. Percutaneous coronary intervention in diabetic patients: a problem? Horm Metab Res 2005;37 (Suppl 1):83–9. [PubMed: 15918116]
3. Iijima R, Mehilli J, Schömig A, Kastrati A. Clinical evidence on polymer-based sirolimus and paclitaxel eluting stents. Minerva Cardioangiol 2006;54:539–55. [PubMed: 17019392]
4. Agostoni P, Valgimigli M, Abbate A, Cosgrave J, Pilati M, Biondi-Zoccai GG. Is late luminal loss an accurate predictor of the clinical effectiveness of drug-eluting stents in the coronary arteries? Am J Cardiol 2006;97:603–5. [PubMed: 16490421]
5. Pfisterer M, Brunner-La Rocca HP, Buser PT, et al. BASKET-LATE Investigators. Late clinical events after clopidogrel discontinuation may limit the benefit of drug-eluting stents: an observational study of drug-eluting *vs* bare-metal stents. J Am Coll Cardiol 2006;48:2584–91. [PubMed: 17174201]
6. Finn AV, Joner M, Nakazawa G, et al. Pathological correlates of late drug-eluting stent thrombosis: strut coverage as a marker of endothelialization. Circulation 2007;115:2435–41. [PubMed: 17438147]

7. Scheller B, Speck U, Abramjuk C, Bernhardt U, Böhm M, Nickenig G. Paclitaxel balloon coating, a novel method for prevention and therapy of restenosis. Circulation 2004;110:810–4. [PubMed: 15302790]
8. Scheller B, Hehrlein C, Bocksch W, et al. Treatment of coronary in-stent restenosis with a paclitaxel-coated balloon catheter. N Engl J Med 2006;255:2113–24. [PubMed: 17101615]
9. Charles R, Sandirasegarane L, Yun J, et al. Ceramide-coated balloon catheters limit neointimal hyperplasia after stretch injury in carotid arteries. Circ Res 2000;87:282–8. [PubMed: 10948061]
10. Bourbon NA, Sandirasegarane L, Kester M. Ceramide-induced inhibition of Akt is mediated through protein kinase Czeta: implications for growth arrest. J Biol Chem 2002;277:3286–92. [PubMed: 11723139]
11. Stover T, Kester M. Liposomal delivery enhances short-chain ceramide-induced apoptosis of breast cancer cells. J Pharmacol Exp Ther 2003;307:468–75. [PubMed: 12975495]
12. Bourke SL, Kohn J. Polymers derived from the amino acid L-tyrosine: polycarbonates, polyarylates and copolymers with poly(ethylene glycol). Adv Drug Deliv Rev 2003;55:447–66. [PubMed: 12706045]
13. Weber N, Wendel HP, Kohn J. Formation of viscoelastic protein layers on polymeric surfaces relevant to platelet adhesion. J Biomed Mater Res A 2005;72:420–7. [PubMed: 15678483]
14. Bowyer JF, Pogge AR, Delongchamp RR, et al. A threshold neurotoxic amphetamine exposure inhibits parietal cortex expression of synaptic plasticity-related genes. Neuroscience 2007;144:66–76. [PubMed: 17049170]
15. Maley D, Mei J, Lu H, Johnson DL, Ilyin SE. Multiplexed RT- PCR for high throughput screening applications. Comb Chem High Throughput Screen 2004;7:727–32. [PubMed: 15578934]
16. Livak KJ, Schmittgen TD. Analysis of relative gene expression data using real-time quantitative PCR and the 2(−Delta Delta C(T)) Method. Methods 2001;25:402–8. [PubMed: 11846609]
17. Merrill AH Jr, Sullards MC, Allegood JC, Kelly S, Wang E. Sphingolipidomics: high-throughput, structure-specific, and quantitative analysis of sphingolipids by liquid chromatography tandem mass spectrometry. Methods 2005;36:207–24. [PubMed: 15894491]
18. Fox TE, Han X, Kelly S, et al. Diabetes alters sphingolipid metabolism in the retina: a potential mechanism of cell death in diabetic retinopathy. Diabetes 2006;55:3573–80. [PubMed: 17130506]
19. Johns DG, Webb RC, Charpie JR. Impaired ceramide signalling in spontaneously hypertensive rat vascular smooth muscle: a possible mechanism for augmented cell proliferation. J Hypertens 2001;19:63–70. [PubMed: 11204306]
20. Gomez-Munoz A. Ceramide 1-phosphate/ceramide, a switch between life and death. Biochim Biophys Acta 2006;1758:2049–56. [PubMed: 16808893]
21. Tang L, Eaton JW. Fibrin(ogen) mediates acute inflammatory responses to biomaterials. J Exp Med 1993;178:2147–56. [PubMed: 8245787]
22. Olivera A, Buckley NE, Spiegel S. Sphingomyelinase and cell-permeable ceramide analogs stimulate cellular proliferation in quiescent Swiss 3T3 fibroblasts. J Biol Chem 1992;267:26121–7. [PubMed: 1464623]
23. Alewijnse AE, Peters SL, Michel MC. Cardiovascular effects of sphingosine-1-phosphate and other sphingomyelin metabolites. Br J Pharmacol 2004;143:666–84. [PubMed: 15504747]
24. Romiti E, Meacci E, Tani M, et al. Neutral/alkaline and acid ceramidase activities are actively released by murine endothelial cells. Biochem Biophys Res Commun 2000;275:746–51. [PubMed: 10973793]
25. Rajesh M, Kolmakova A, Chatterjee S. Novel role of lactosylceramide in vascular endothelial growth factor-mediated angiogenesis in human endothelial cells. Circ Res 2005;97:796–804. [PubMed: 16151023]
26. Gouaze-Andersson V, Cabot MC. Glycosphingolipids and drug resistance. Biochim Biophys Acta 2006;1758:2096–103. [PubMed: 17010304]
27. Furuya K, Ginis I, Takeda H, Chen Y, Hallenbeck JM. Cell permeable exogenous ceramide reduces infarct size in spontaneously hypertensive rats supporting *in vitro* studies that have implicated ceramide in induction of tolerance to ischemia. J Cereb Blood Flow Metab 2001;21:226–32. [PubMed: 11295877]

28. Lightle S, Tosheva R, Lee A, et al. Elevation of ceramide in serum lipoproteins during acute phase response in humans and mice: role of serine-palmitoyl transferase. Arch Biochem Biophys 2003;419:120–8. [PubMed: 14592455]

29. Hammad SM, Taha TA, Nareika A, Johnson KR, Lopes-Virella MF, Obeid LM. Oxidized LDL immune complexes induce release of sphingosine kinase in human U937 monocytic cells. Prostaglandins Other Lipid Mediat 2006;79:126–40. [PubMed: 16516816]

30. Siess W. Athero- and thrombogenic actions of lysophosphatidic acid and sphingosine-1-phosphate. Biochim Biophys Acta 2002;1582:204–15. [PubMed: 12069830]

31. Li XA, Titlow WB, Jackson BA, et al. High density lipoprotein binding to scavenger receptor, Class B, type I activates endothelial nitric-oxide synthase in a ceramide-dependent manner. J Biol Chem 2002;277:11058–63. [PubMed: 11792700]

32. Xia P, Vadas MA, Rye KA, Barter PJ, Gamble JR. High density lipoproteins (HDL) interrupt the sphingosine kinase signaling pathway: A possible mechanism for protection against atherosclerosis by HDL. J Biol Chem 1999;274:33143–7. [PubMed: 10551885]

33. Worgall TS, Johnson RA, Seo T, Gierens H, Deckelbaum RJ. Unsaturated fatty acid-mediated decreases in sterol regulatory element-mediated gene transcription are linked to cellular sphingolipid metabolism. J Biol Chem 2002;277:3878–85. [PubMed: 11707431]

34. Lemos PA, Serruys PW, Sousa JE. Drug-eluting stents: cost *vs* clinical benefit. Circulation 2003;107:3003–7. [PubMed: 12821586]

35. Kaiser C, Brunner-La Rocca HP, Buser PT, et al. BASKET Investigators. Incremental cost-effectiveness of drug-eluting stents compared with a third-generation bare-metal stent in a real-world setting: randomised Basel Stent Kosten Effektivitats Trial (BASKET). Lancet 2005;366:921–9. [PubMed: 16154019]

36. Speck U, Scheller B, Abramjuk C, et al. Neointima inhibition: comparison of effectiveness of non-stent-based local drug delivery and a drug-eluting stent in porcine coronary arteries. Radiology 2006;240:411–8. [PubMed: 16864669]

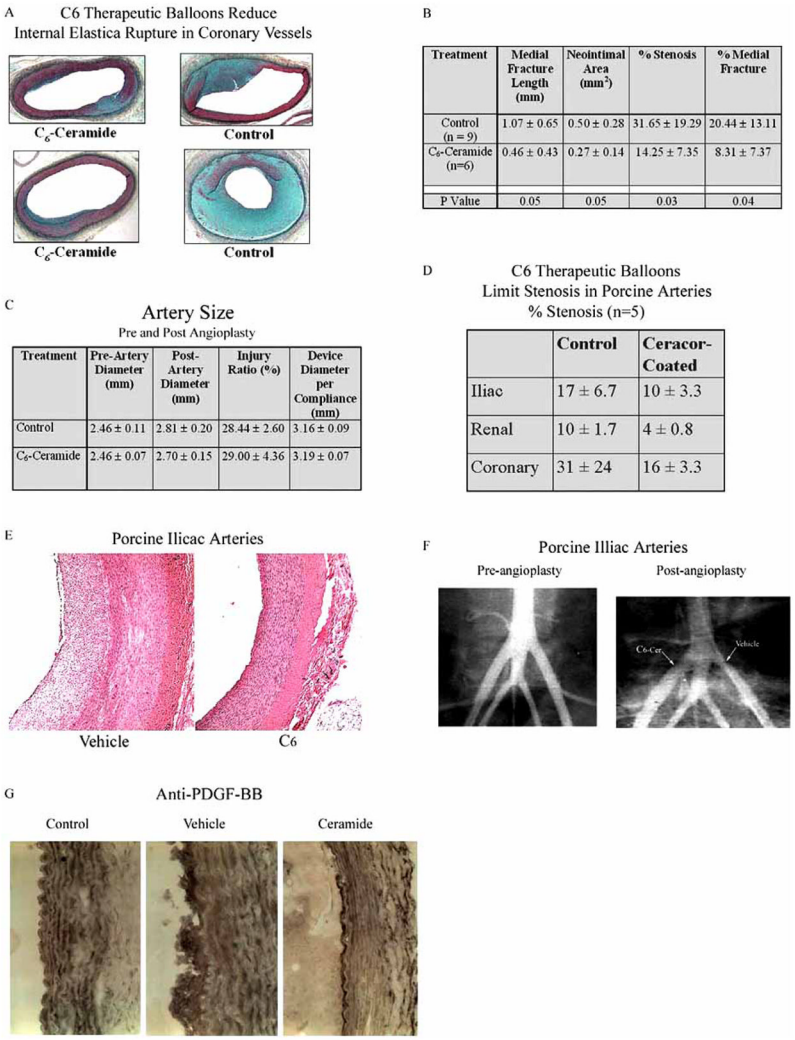

Fig. 1. C_6-Ceramide-therapeutic balloons reduce stenosis in multiple arterial beds in both porcine and rabbit models of stretch injury

A) C_6-Ceramide-therapeutic balloons reduced internal elastica injury with a corresponding reduction in medial fracture length in porcine coronary vessels. Two representative photomicrographs from surgeries performed at Lychron, Inc. **B/C**) Quantification of percent stenosis and percent medial fracture of n = 6–9 pigs (B) and quantification of pre- and post-angioplasty diameters of experimental animals (**C**). **D**) C_6-ceramide-therapeutic balloons limited stenosis in porcine iliac, renal, and coronary arteries. Quantification of percent stenosis, n = 5 pigs. Surgeries performed at Penn State College of Medicine. **E/F**) Representative photomicrograph of H & E stained sections (**E**) and radiological image (**F**) of porcine iliac arteries treated with C_6-ceramide-therapeutic balloons. **G**) C_6-ceramide-therapeutic balloons promote re-endothelialization of rabbit carotid arteries. Increased endothelial cell PDGF-ββ expression was observed three days after treatment with C_6- but not vehicle-treated balloons. Representative photomicrograph of n = 3 separate experiments.

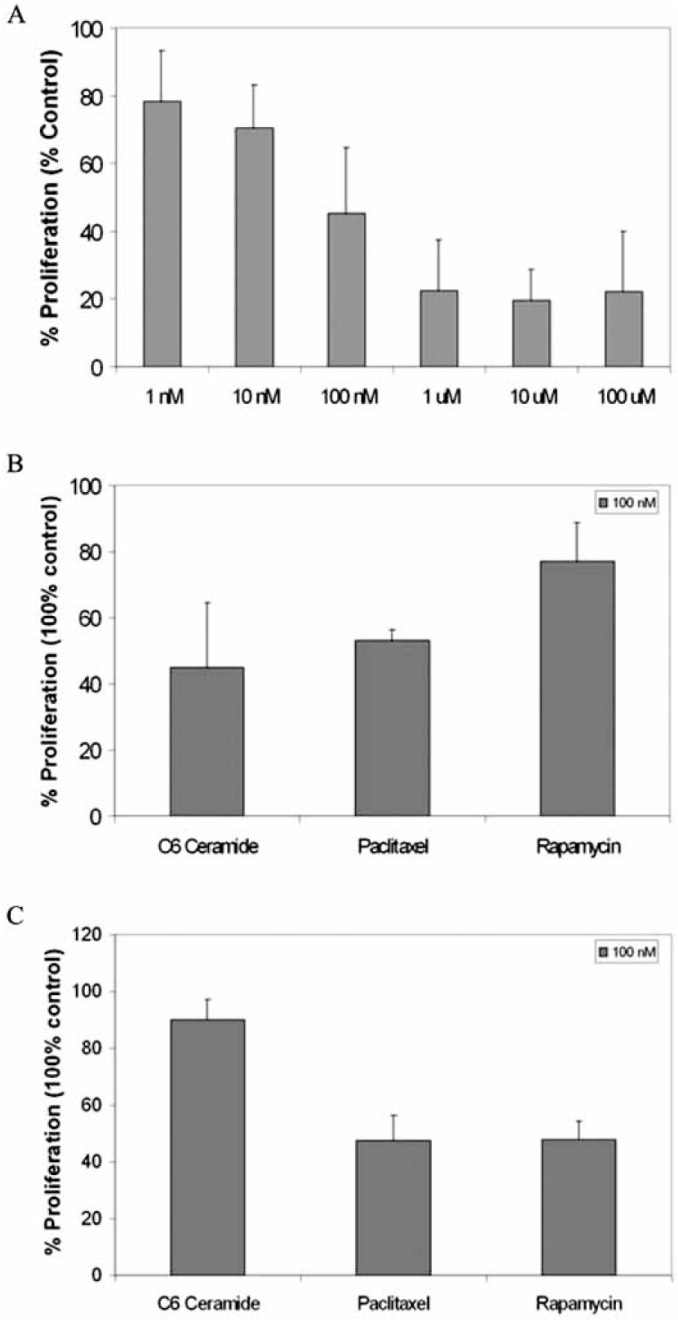

Fig. 2. C_6-ceramide preferentially decreases human coronary artery smooth muscle cell (HCASMC) proliferation but not human coronary artery endothelial cell (HCAEC) proliferation

A) C_6-ceramide decreases HCASMC proliferation as a function of dose. In n = 3 experiments, C_6-ceramide, at a concentration of 100 nmol/L, decreases DNA synthesis by approximately 50% in HCASMC as determined *via* ^{3}H-Thymidine incorporation. **B**) C_6-ceramide, at its EC_{50} concentration, decreases HCASMC proliferation more than paclitaxel and rapamycin at equivalent concentrations, n = 3. C) Paclitaxel and rapamycin, but not C_6-ceramide, limit HCAEC proliferation. Thymidine incorporation into HCAEC acid-insoluble DNA is less for paclitaxel and rapamycin, as compared to 100 nmol/L C_6-ceramide, n = 3.

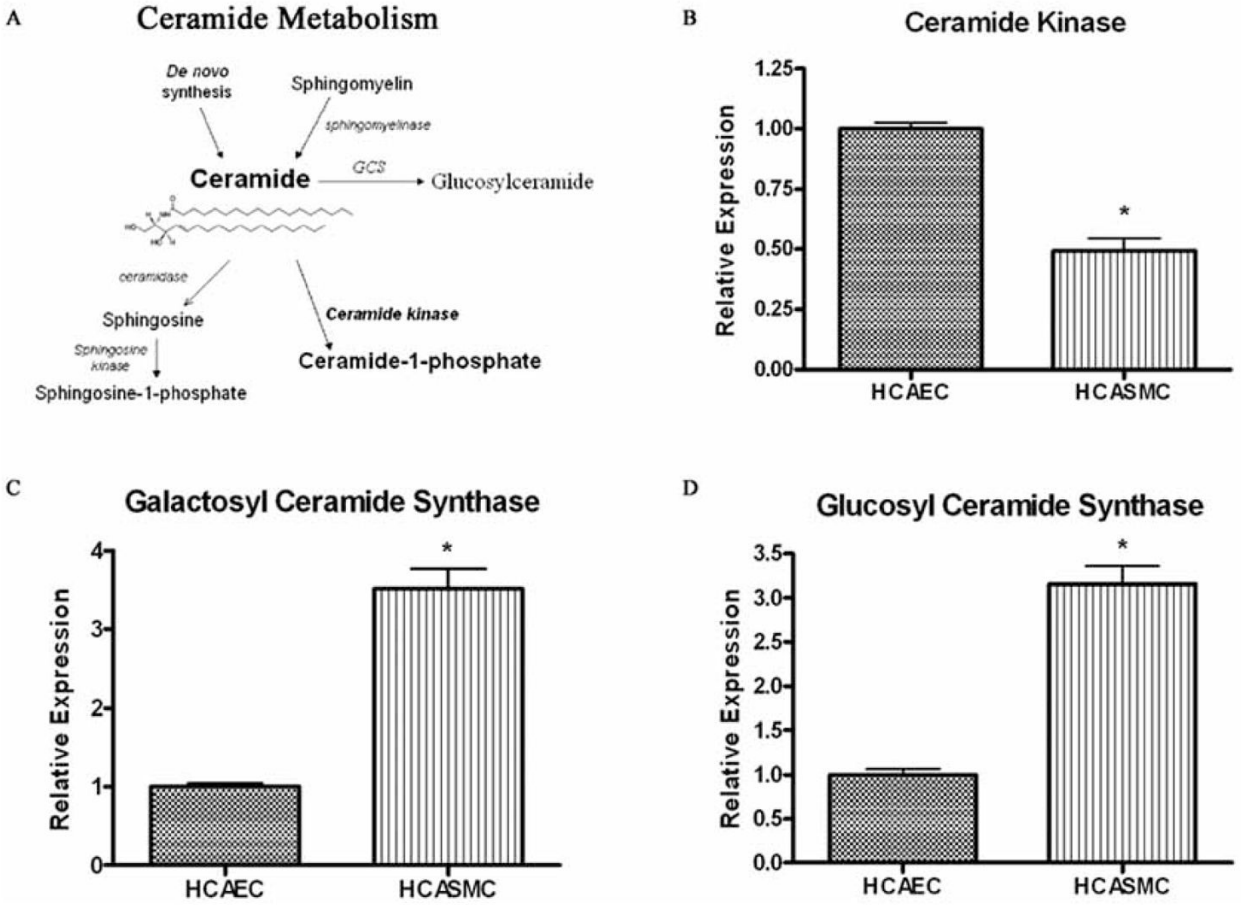

Fig. 3. Human coronary artery endothelial cells have an increased capacity to metabolize ceramide into phosphorylated, but not glycosylated, metabolites

(**A**) Primary ceramide metabolic pathways. The dynamic flux of ceramide metabolites regulates the switch between apoptosis/growth arrest and proliferation. Anti-apoptotic/proliferative phosphorylated metabolites are formed *via* ceramide kinase or sphingosine kinase. The galactosyl- and glucosylceramide synthases (GCS) metabolize ceramide into less bioactive glycosylated ceramide species. (**B-D**) Gene expression of sphingolipid metabolic enzymes ceramide kinase (**B**), galactosylceramide synthase (**C**), and glucosylceramide synthase (**D**), in human coronary artery endothelial cells (HCAEC) and smooth muscle cells (HCASMC) was measured by real time RT-PCR. Enzyme mRNA expression levels are all relative to their respective level in vehicle treated HCAECs, (mean ± SEM, $n \geq 5$); * Denotes significance compared to vehicle treated HCAECs.

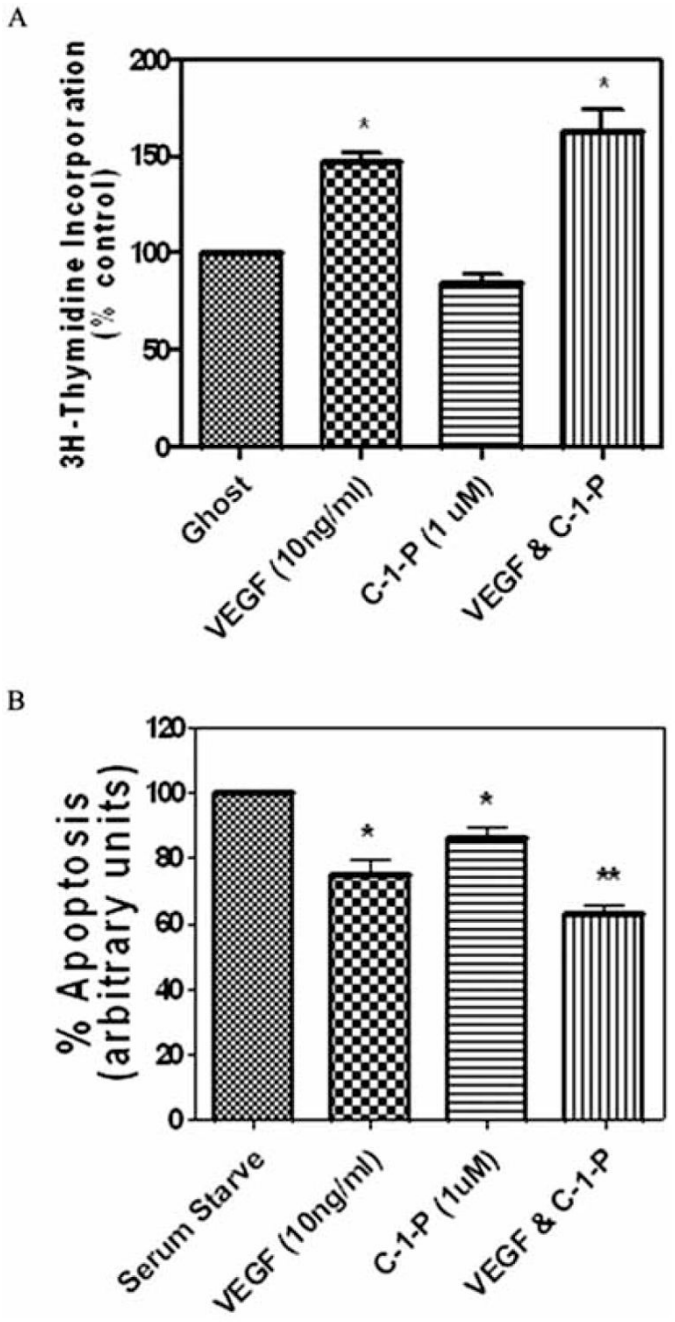

Fig. 4. C_8 –Ceramide-1-Phosphate (C_8 –C-1-P) enhances VEGF induced human coronary artery endothelial cell survival but not proliferation

(**A**) C_8–C-1-P (1 μmol/L) did not enhance VEGF-induced (10 ng/μL) HCAEC proliferation as determined *via* ^{3}H-thymidine incorporation, n = 6 separate replicative experiments. (**B**) C_8–C-1-P (1 μmol/L) attenuated apoptosis (caspase 3/7 activity) in serum-deprived HCAEC. In addition, C_8–C-1-P enhanced VEGF-induced (10 ng/μL) attenuation of apoptosis in serum-deprived HCAEC, n = 5. * Denotes significance compared to serum starved HCAEC's. ** Denotes significance compared to serum starved HCAEC's treated with VEGF, p=.05.

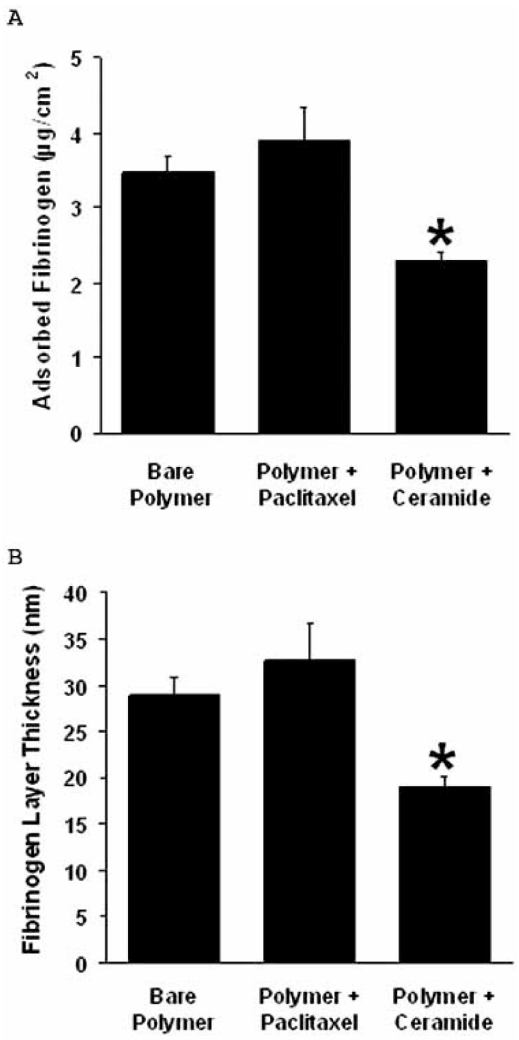

Fig. 5. C_6-ceramide modifies the formation of the fibrin matrix

Fibrinogen adsorption to C_6-ceramide-coated films was decreased compared to paclitaxel-coated or bare films. (**A**) A smaller mass of fibrinogen was adsorbed on C_6-ceramide coated polymer films than on paclitaxel-coated or bare films. (**B**) Surface-adsorbed fibrinogen mass was used to calculate fibrinogen layer thickness on polymer films according to the Voight model (according to reference [12]), n = 3.

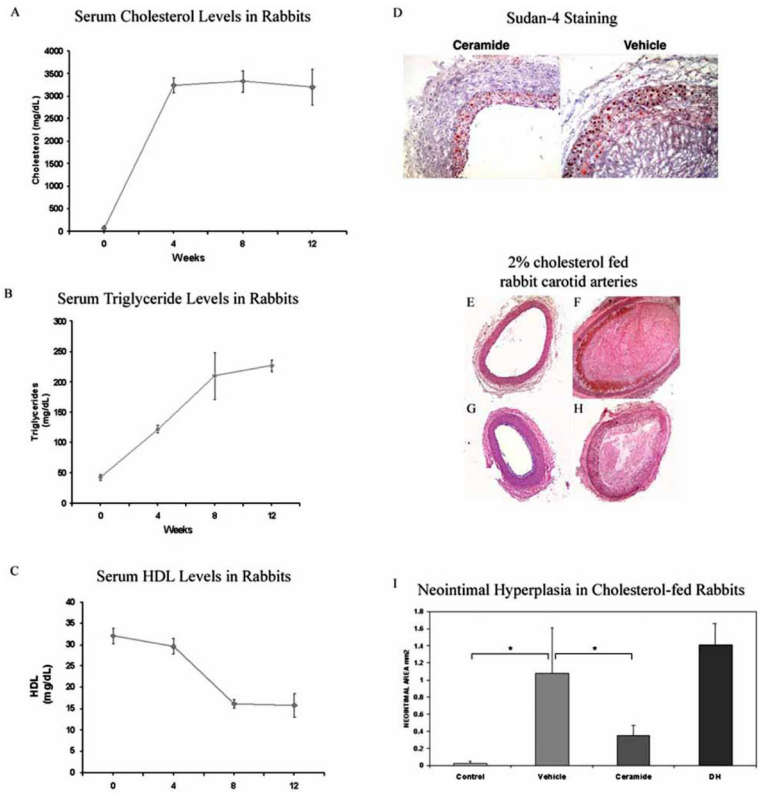

Fig. 6. C_6-Ceramide-therapeutic balloons limit carotid artery positive remodeling, thrombosis, as well as neointimal hyperplasia in a cholesterol-fed rabbit model of hyperlipidemia

(**A–C**) Serum cholesterol (**A**), triglyceride (**B**), and HDL (**C**) levels in rabbits during a 12 week diet of 2% cholesterol, n = 6. Cholesterol and triglyceride levels were elevated with a concomitant decrease in HDL levels. (**D**) Sudan 4 staining revealed that C_6-ceramide limited the enhanced lipid accumulation within the neointimal and thrombogenic core of the angioplastied carotid arteries, n = 3. (**E–I**) Representative photomicrographs (**E–H**) and quantification (**I**) of arteries from 2% cholesterol fed rabbits show C_6-ceramide therapeutic balloon treatment reduced the degree of positive remodeling and thrombosis at the site of injury. Photomicrographs are of a non-angioplastied artery (**E**), and angioplastied arteries with balloon catheters coated with vehicle (**F**), C_6-ceramide (**G**), or inactive dihydro-C_6-ceramide (**H**). C_6-ceramide coated, but not dihydro-C_6-ceramide coated, balloon catheters decreased the post-angioplasty neointimal area of arteries in hyperlipidemic rabbits, n = 6 animals.

Table 1

Lipodomic Profile of Basal and C_6-Ceramide-Treated Human Coronary Artery Smooth Muscle Cells and Human Coronary Artery Endothelial Cells

Treatment	Cell Type	Total Ceramide (pmol/mg protein)	C-1-P (pmol/mg protein)	Cerebrosides (pmol/mg protein)
Vehicle	HCASMC	382.4 ± 28.5	5.87 ± 0.95	330.50 ± 44.02
	HCAEC	270.6 ± 17.2	4.55 ± 0.88	***19.68*** ± 4.20
C_6-Ceramide	HCASMC	8207.8 ± 438.8	9.02 ± 1.30	4070.30 ± 480.60
	HCAEC	7933.4 ± 59.5	***17.09*** ± 2.67	***680.26*** ± 36.85

HCAEC bolded, italicized values differ significantly ($p<0.05$) compared to HCASMC with respective treatment, n = 9–10 separate replicate experiments.

Table 2

C_6-Ceramide Doses in Animals and Humans

Species	Maximum Tolerated C_6-Ceramide Concentration	Human Dose Equivalent	Multiple of Expected Clinical Dose (ECD)*
Rat	15 mg/kg	2.43 mg/kg	972
Dog	7.5 mg/kg	4.06 mg/kg	1624

* assumes a human clinical dose =150 μg/60kg.